Ocean Dynamics (2020) 70:231–239
https://doi.org/10.1007/s10236-019-01316-9

Wind and wave height climate from two decades of altimeter records on the Chilean Coast (15°–56.5° S)

Dernis Mediavilla[1,2,3] · Héctor Hito Sepúlveda[4] · Guadalupe Alonso[5]

Received: 13 May 2019 / Accepted: 4 October 2019 / Published online: 27 November 2019

Abstract
In order to look for climatological changes on significant wave height and wind magnitude distributions, two decades of altimeter data were analyzed in a monthly 1° × 1° grid at the Southeastern Pacific Ocean, offshore of Chile. Both wind magnitude and significant wave height shown significant growing medians, at a rate of up to 0.2 m dec^{-1} and 1 m s^{-1} dec^{-1}, respectively. Nevertheless, the shape of both statistical distributions shows regional differences from North to South. We conclude that both significant wave height and wind magnitude distributions experienced significant changes during the last two decades and also that their behavior is not uniform along the Southeastern Pacific Ocean.

Keywords Altimetry · Wind climate · Wave climate · Chile

1 Introduction

The impact of wind and waves on energy, coastal circulation, sediment transport, and infrastructure is an important reason to understand their past and future variability. Variations in the wind and wave climate have been studied from both a historical perspective using data analysis and modeling studies, and future climate change scenarios, using coupled general circulation models (GCM, e.g., Reyers et al. 2016) or statistical approaches (e.g., Wang et al. 2014).

Waves of wind origin (including swell and wind waves) represent a large portion of the energy contained in ocean surface waves, in comparison with tsunamis and tides (Aguirre et al. 2017). They are generally classified depending upon how close are they to the point they were generated. During the development phase, they are refereed as wind sea, being strongly coupled to the local wind field. After waves have traveled a significant distance, so that their phase speed overcomes the wind speed of their generation phase, they are designated as swell, these waves being decoupled from the local wind field at the place of their observation. Wave climatologies have been developed since 1996 (Barstow 1996), and one of the main topics study of the wave field has been the separation of the wind sea and the swell contributions.

The main sources of information for historical studies have been satellite altimetry and satellite scatterometers, with global records starting in the early 1990, model hindcast reanalysis, which rely on numerical wave models and wind hindcast reanalysis, and to a minor extent visual observations from ships or platform. These two sources of information have their own problems. Satellite altimetry information is limited by the spatial and temporal coverage of available remote sensors, as well as the variations on their precision and accuracy. Model hindcast reanalysis depends on the physical parametrizations for the numerical models used, as well as the correct description of the wind reanalysis that is used as the main forcing. Wind reanalysis has

This article is part of the Topical Collection on the *International Conference of Marine Science ICMS2018, the 3rd Latin American Symposium on Water Waves (LatWaves 2018), Medellin, Colombia, 19-23 November 2018 and the XVIII National Seminar on Marine Sciences and Technologies (SENALMAR), Barranquilla, Colombia 22-25 October 2019*

Responsible Editor: Alexander Babanin

✉ Héctor Hito Sepúlveda
andres@dgeo.udec.cl

[1] Graduate Program in Oceanography, Department of Oceanography, University of Concepción, Concepción, Chile

[2] Programa COPAS-Sur Austral, Universidad de Concepción, Concepción, Chile

[3] Present address: Marine Energy Research and Innovation Centre (MERIC), Santiago, Chile

[4] Geophysics Department, Faculty of Physical and Mathematical Sciences, Universidad de Concepción, Concepción, Chile

[5] Servicio de Hidrografía Naval, Armada Argentina, Av. Montes de Oca 2124, C1270ABV Ciudad Autónoma de Buenos Aires, Argentina

known limitations such as underestimation of high wind speeds (ERA-40, Caires and Sterl 2003), or decadal variations on bias (Stopa and Cheung 2014). Visual observation records are an important source of verification for modeling and remote sensing efforts; however, they are limited in their spatial coverage, particularly in the Southern Hemisphere.

It has been found that the wave field is dominated by swell, even in areas where wind sea is important (Semedo et al. 2011). Positive linear trends in Hs of up to 20 cm dec^{-1} have been observed in the North Atlantic and North Pacific (Semedo et al., 2011). These trends have been found for wind speed and wave height in other studies (Young et al. 2011) using 23 years of satellite altimetry data. A more recent analysis covering the 1985–2018 period is also discussed by Young and Ribal (2019). In all cases, the length of the time series does not allow yet to distinguish whether such variations are a trend or part of a multi-decadal oscillation (Young et al. 2011; Young and Ribal 2019). The increasing trend is more statistically significant for extreme than for mean monthly values. In the Southern Hemisphere, Hs trends present a positive correlation with the Southern Annular Mode (SAM, Hemer et al. 2010), and similar connection to atmospheric patterns has been observed in the North Atlantic (e.g., Kushnir et al. 1997).

2 Data and methods

Wave height and wind speed altimeter data from a merged and calibrated data set, regularly updated, based on the GLOBWAVE database (Queffeulou 2013; Queffeulou and Croizé-Fillon 2013) were extracted, spanning the years 1993 to 2012 for the region from 15° S to 56.5° S and 81° W up to 69° W (Fig. 1). A 1° × 1° grid and monthly temporal resolution were chosen for the analysis, in order to account for a statistically large amount of data per cell (not less than 30 measurements) to estimate the median, skewness, and kurtosis of the significant wave height (Hs) and wind speed (Ws). Therefore, a monthly, one degree resolution database was constructed for the median, kurtosis, and skewness from the observations of Hs and Ws. From the two-decade time series, the 99 percentile was estimated per cell when the cell had more than 800 satellite observations in this 19-year period. Also, a seasonal analysis was performed (JJA, Southern Hemisphere winter), building a time series of the median of those cells with at least 90 measurements per season. Finally, climatological seasonal fields are shown of the two-decade observations of Ws and Hs.

Focusing on general statistical descriptors, the main goal of this work is to look for climatological changes on Hs and Ws distributions. The statistical descriptors used are the median, skewness, kurtosis, and 99th percentile. The *median* accounts for the 50th percentile value, providing an estimate of the distribution shift towards higher or lower values. Distribution

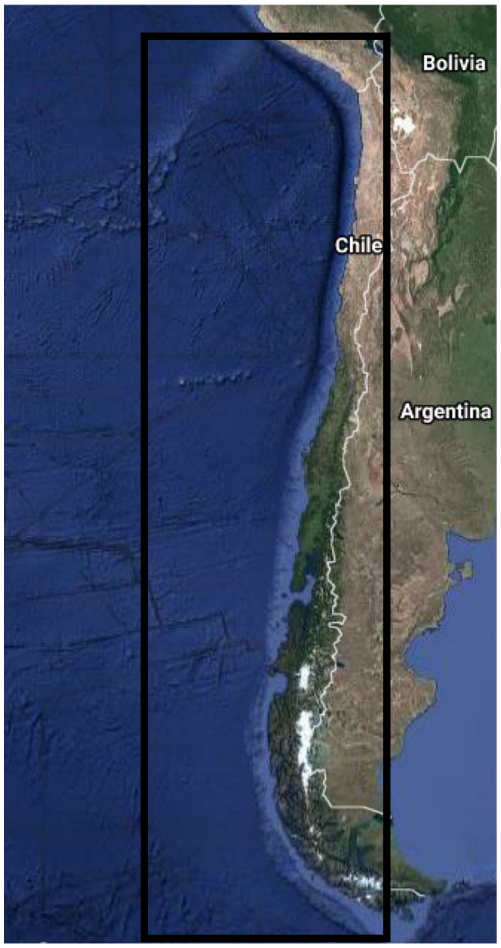

Fig. 1 Study area. The region selected for the study is delimited with a black line

skewness is a measure of the asymmetry of the time series, indicating whether the values are gathered amongst lower (left shifted distribution, negative value) or higher values (right shifted distribution, positive value). By definition, the skewness of a distribution is

$$s = \frac{E(\chi - \mu)^3}{\sigma^3} \tag{1}$$

where μ is the mean and σ is the standard deviation of the time series, and $E(t)$ represents the expected value of the quantity t. Here, it is obtained by

$$s = \frac{\frac{1}{n}\sum_{i=1}^{n}\left(x_i - \overline{x}\right)^3}{\left(\sqrt{\frac{1}{n}\sum_{i=1}^{n}\left(x_i - \overline{x}\right)^2}\right)^3} \tag{2}$$

where n is the length of the time series and $\overline{x}$ is the mean.

On the other hand, the *kurtosis* is a measure of how outlier-prone a distribution is. Meaning, in other words, how disperse or built up the values are. It is defined as

$$k = \frac{E(x-\mu)^4}{\sigma^4} \tag{3}$$

And, it is applied by the equation

$$k = \frac{\frac{1}{n}\sum_{i=1}^{n}\left(x_i-\overline{x}\right)^4}{\left(\frac{1}{n}\sum_{i=1}^{n}\left(x_i-\overline{x}\right)^2\right)^2} \tag{4}$$

Finally, the *99th percentile* (meaning 99th percentile of the measurements are found below that value, and, the same way, that only 1% of the data exceeded it) gives information about the position of the higher "tail" of the distribution, and so, of the extreme values.

The main objective of this work is to investigate climatological changes on Hs and Ws for the region, by analyzing the possible trends in gridded altimeter data. In order to do so, it is necessary to determine the magnitude of any monotonic trend present in the data and whether it is statistically significant. In this regard, Young et al. (2011) evaluated a number of different techniques for the determination of the trend. They concluded that the Seasonal Kendall test recovers the trend most accurately. The Seasonal Kendall test (Hirsch et al. 1982) accounts for seasonality by computing the Mann Kendall test on each season separately, and then combining the results. Following Young et al. (2011), the Seasonal Kendall test with a significance of 95% was used to compute the trends. First, the trend of each statistical descriptor was calculated in every cell with no more than 25% of missing data. Secondly, seasonal values of Hs and Ws were obtained for each of the cells with more than 90 measurements per season. The same trend analysis as before was applied with a confidence level of 95%. Also, seasonal characteristic fields were obtained as well for each variable (considering the two decade time series for each cell).

3 Results

Two-decade monthly series of median Ws and Hs are first analyzed. Sen's slope of the monthly median series is shown in Fig. 2. This trend is not homogeneous from North to South in the Southeastern Pacific Ocean region. Significantly positive median trends are found in Northern Chile, both in Hs and Ws, up to 35° S, followed by a non-significant trend region, that ends around 45° S, where the median trend shows positive values again. Positive median slopes imply that in the last 20 years, both Hs and Ws have been growing, up to 0.2 m dec^{-1} and 1 m s^{-1} dec^{-1}, respectively. This means that the center of the distribution (50th percentile) shifted towards higher values. Considering this latitudinal trend differences, we proposed a regional approach for the analysis (regions delimited on Fig. 2). Note that there are no significant negative slopes in the studied area, but rather both North and South Regions tend to have higher Hs and Ws this last two decades.

Two other statistical descriptors were analyzed in order to see if the change in the median indicates a uniform shift of Hs and Ws towards higher values, or if the shape of the distribution showed significant modifications during time. Kurtosis and skewness 20-year slopes per cell are displayed in Fig. 3. Results showed a shift towards a more gathered Ws distribution, mainly towards higher values in the Central Region, and towards lower ones in the North (where the kurtosis and skewness slopes are highly significant) and South Regions. At the Central and South Regions, Hs distributions follow the trend of Ws. On the other hand, the Northern Region presents an opposite kurtosis and skewness trends for Hs and Ws, showing waves that tend to have a more evenly distributed significant height, with magnitudes growing towards lower values.

Considering these results, we can conclude that both significant wave height and wind magnitude distributions experienced significant changes during the last two decades, and also that their behavior is not uniform along the Chilean coast. In order to explore further the nature of this changes, a seasonal analysis was performed.

Figure 4 displays linear trends obtained for each season of median Hs, along with the seasonal climatological mean fields. Latitudinal differences in seasonal Hs estimations are evident. The South Region shows the highest Hs values, growing over the last two decades. Nevertheless, the Summer (DJF) is the only season that shows significant positive trends, being possibly the season responsible for the median growth mentioned earlier (cf. Fig. 2). The North Region, presenting the lowest Hs through the year, shows a dichotomous trend, with Hs significantly augmenting in Autumn (MAM) and Winter (JJA) and descending less significantly in Summer (DJF). Positive trends exceed then the negative Summer trend, leading to the global increment of the Hs median found in the North Region. On the other hand, the Central Region appears to be a transition Region, with waves of 2.5 m in its southern limit in Summer that reach its northern limit in Winter, and no definite trend, consistent with the global trend shown in the monthly median Hs series.

This meridional contrast, with high *Hs* in the South and low in the North, is present also in the extreme latitudinal distribution. Figure 5 shows the estimation of 99th percentile for *Hs* median, meaning that only 1% of the data obtained by the altimeter per monthly 1° × 1° cell exceeds those values. In the figure, the closest location to seven of the most important Chilean harbors is highlighted, along with the number of events that exceeds the 99th percentile of *Hs*. The *Hs* exceeded 3.67 m during the last 20 years 189 times in Iquique, and up to 139 events of *Hs* higher than 4.66 m were registered in Valparaiso. Offshore of Punta Arenas (South Region, Magellan Strait), 130 times the *Hs* was over almost 8 m.

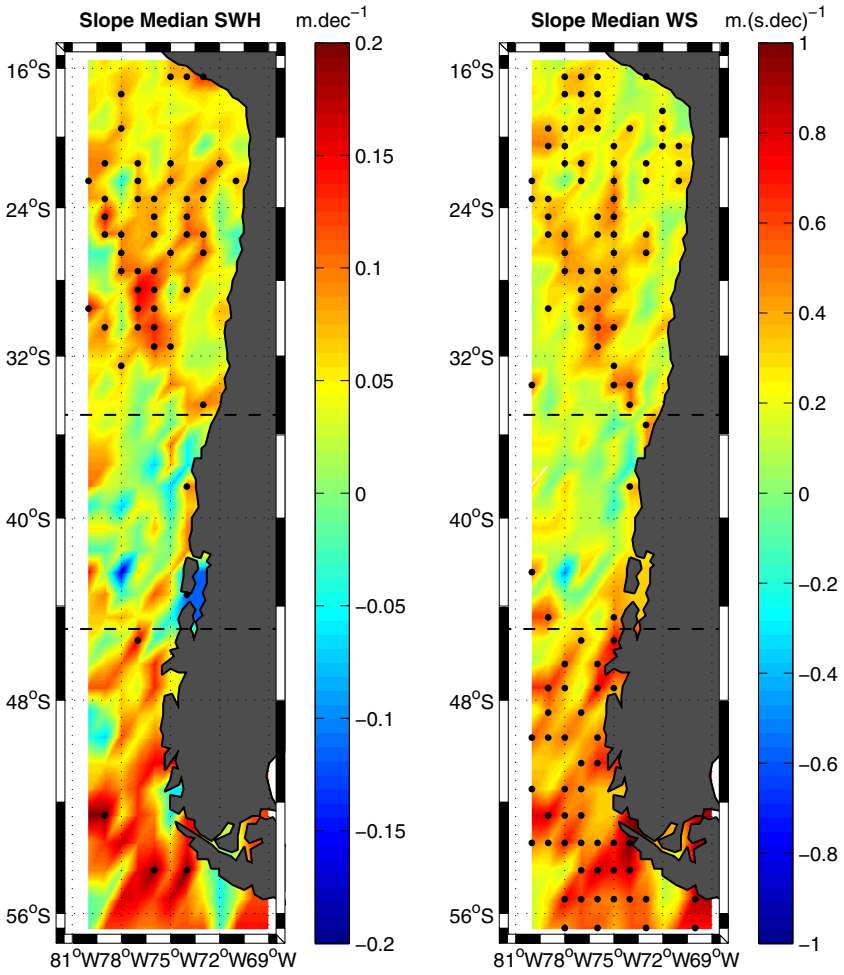

Fig. 2 Seasonal Mann Kendalls Sen's Slope of the monthly median series for Hs (**a**) and Ws (**b**). Black dots point the values that are statistically significant (p value ≤ 0.05). Regions suggested for analysis are differentiated by dashed black lines

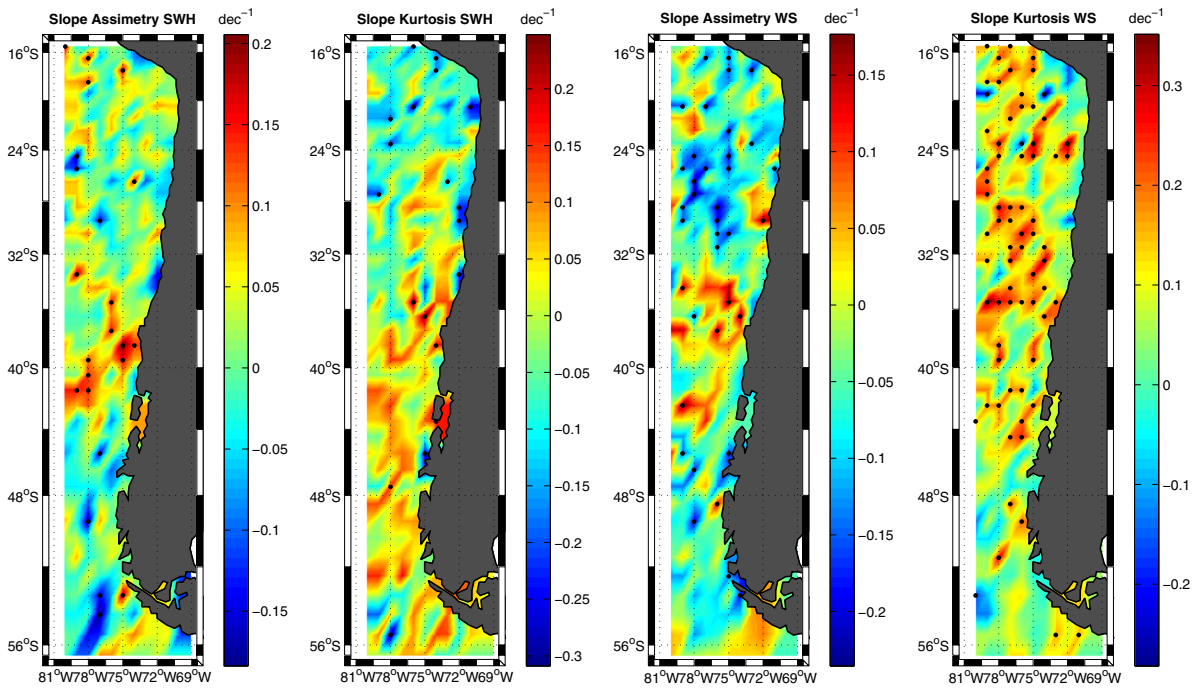

Fig. 3 Skewness and kurtosis slopes for Hs (left) and Ws (right) distributions fields

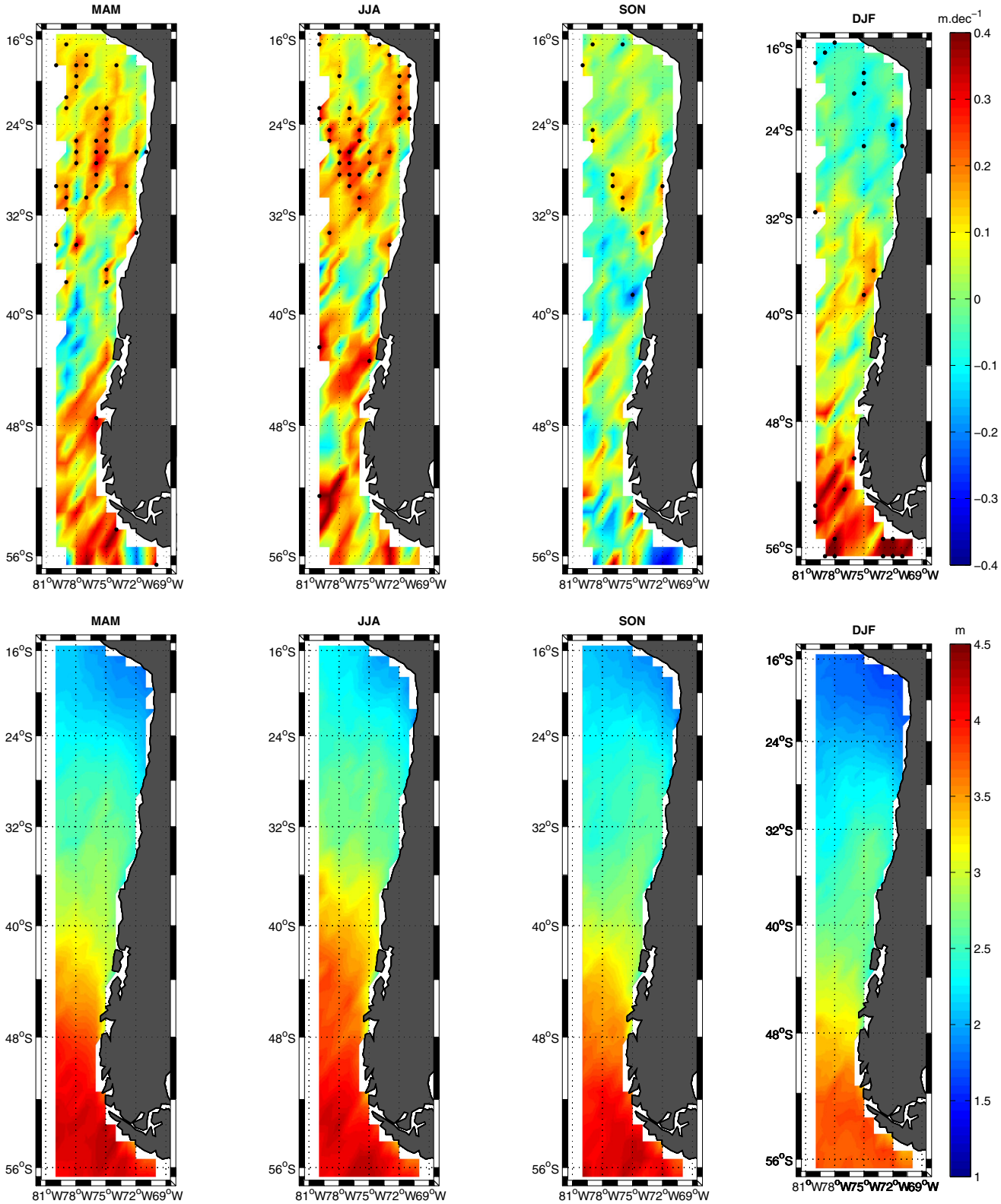

Fig. 4 Hs median seasonal slopes; p values ≤ 0.05 are remarked in black dots (up) and seasonal means for Hs (down)

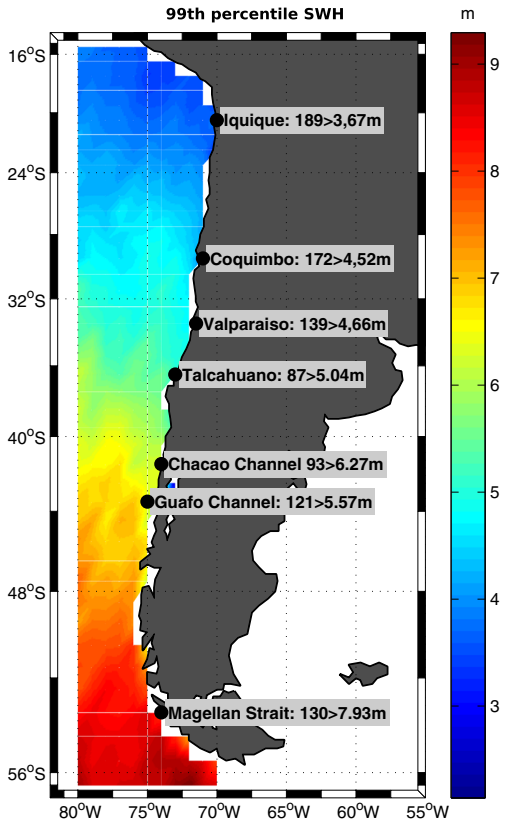

Fig. 5 Hs 99th percentile. showing also its value for the nearest cell of seven principal harbors, along with the number of events represented by this percentile

Wind magnitude seasonal median (Fig. 6) presents also latitudinal differences, with features near the coast that are present through all seasons. Minimum Ws is found in the Northeastern zone of the North Region, displaying significant changes during the cold seasons this last two decades. Wind magnitude outside of this area grew from Autumn to Spring, leading to the global positive trend found in the North Region. High winds in the South Region increased their magnitude in Summer and Autumn. It is worth noting that the North Region shows a local maximum between 30° and 35° S near the coast, with wind magnitudes that increased during Summer and Autumn, synchronized with the South Region seasonal trends. Central Region does not show a dominant seasonal trend, with only few cells with significantly low positive trend in Winter and negative in Spring.

Moreover, both local features in the North Region (the northeastern minimum and ~ 30° S maximum) are highlighted in a 99th percentile analysis, estimated from the two-decade time series (Fig. 7). The lowest winds are located at North Chile, with only 1% of the Ws exceeding 10 m s^{-1} at most, and a magnitude gradient directed perpendicularly to the coast. The local maximum near the coast around 30° S has a north-south orientation, following the coast, with winds lower than 16 m s^{-1} 99% of the time. On the other hand, both Central and South Regions show a more zonally uniform 99th percentile distribution, finding the maximum regional Ws values in the South, with extreme winds that can exceed 20 m s^{-1}.

4 Discussion and conclusion

The correspondence between wind and wave median trends (Fig. 2) possibly is not by chance. Significant wave height accounts for both swell and sea wave contribution to the wave spectra. Hence, it is reasonably to expect that Hs tends to be higher responding to Ws growth in time. In this context, the significance of North and South Region trends is not the same, being higher at the first than at the latter. This is found most likely due to the swell presence in the Southern Ocean that has no direct dependence on local winds but is more related to distant storm tracks. Semedo et al. (2011), following Chen et al. (2002) and Gulev and Grigorieva (2006), show that the global field is dominated by swell waves, finding also that the wave climate variability is also dominated by changes in swell waves carrying the effect of changes in surface winds to large and remote areas. Therefore, the connection between the climatological changes in wind speed and significant wave heights is not necessary direct, due to the arrival of remotely generated waves.

From seasonal Hs, analysis (Fig. 3) is worth noting, on the one hand, that *Hs* median shows a tendency to decrease meridional *Hs* gradient this last two decades during cold seasons, by means of an increment on its magnitude in the region with lower *Hs* (North), with no significant variances on the South. On the other hand, latitudinal differences tend to increase during Summer, with high *Hs* growing in the South and lower *Hs* decreasing in the North.

Young and Ribal (2019) binned the data in a 2° × 2° grid and calculated the mean, mode, and 90 percentile values. In Young and Ribal (2019), most of the quantitative results are expressed for large geographical areas, and the values expressed for our region of interest could be obtained for what is described as the Pacific Ocean or Southern Ocean areas. Keeping this in mind, we choose to mention the values described for both areas. For the area on interest in this manuscript, Young and Ribal (2019) describe a statistically significant increase in mean wave height, and a small decrease in mean wave height for some areas of the Pacific Ocean. By looking close to our area of interest in their Fig. 2, we can recognize a pattern for mean Hs trends where the upper region of the Chilean coast has positive trend values, the middle (~ 40° S) region has some trend values close to 0 or even negative values, and the region below ~ 40° S has larger positive trend values. This agrees in a qualitative way with what we show in our Fig. 2, where three different regions are defined. In absolute values, Young and Ribal (2019) limit their mean and 90 percentile trend scale for Hs to ± 1.0 cm

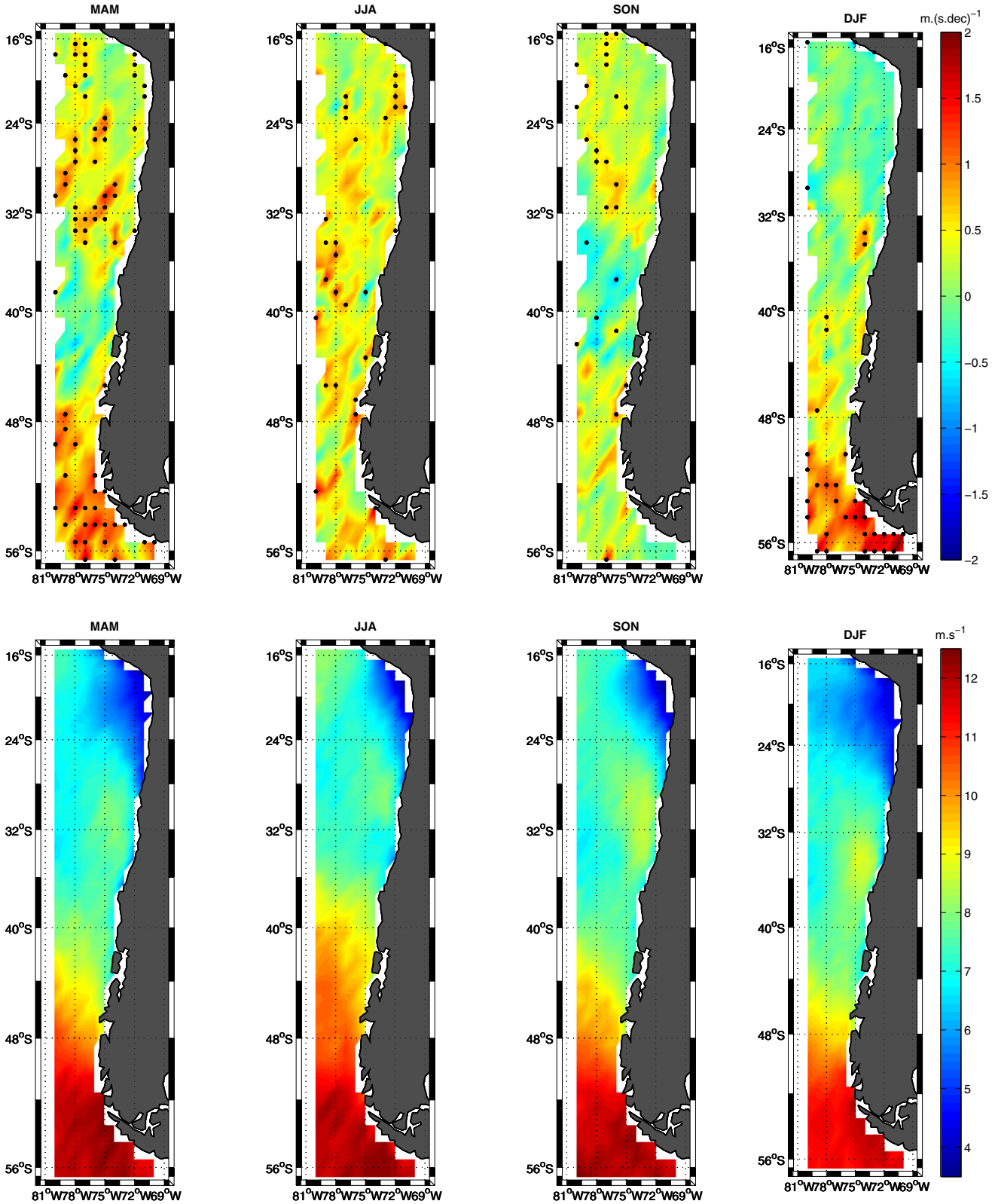

Fig. 6 Ws median seasonal slopes; p values ≤ 0.05 are remarked in black dors (up) and seasonal means for Ws (down)

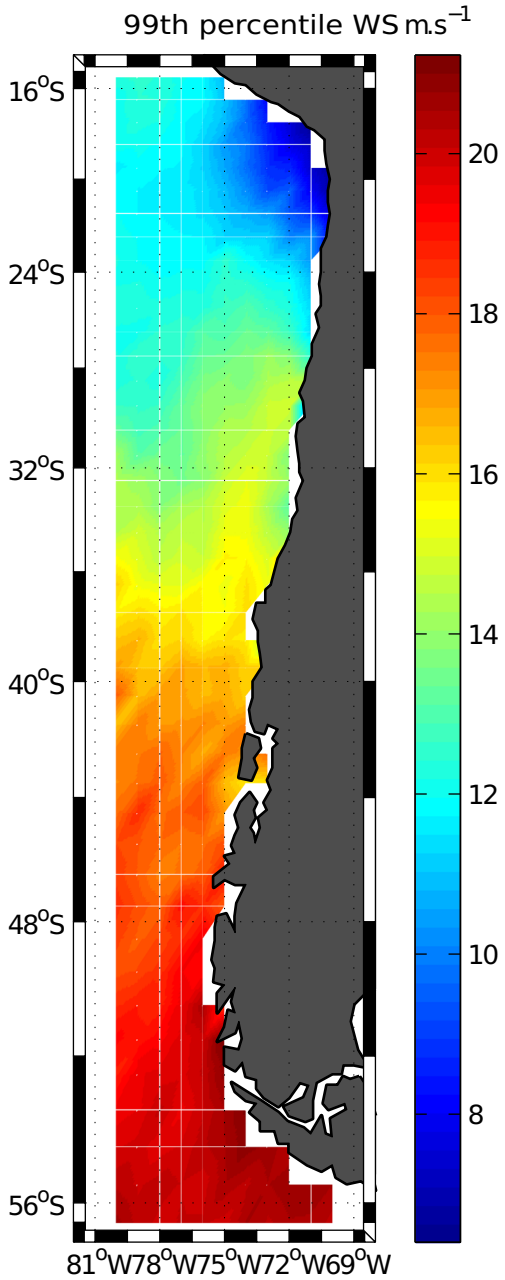

Fig. 7 Ws 99th percentile estimated from the two-decade median time series

year^{-1}, which would be equivalent to 0.1 m dec^{-1} (the units we choose to describe our results, Fig. 2a). This upper value is 50% lower to what we obtain, 0.2 m dec^{-1}. When we compare results for U10, mean and p90 trend values in Young and Ribal (2019) range between ± 6 cm s^{-1} year^{-1} (± 0.6 m s^{-1} dec^{-1} in our chosen units). This would be 40% lower than the values we obtained (Fig. 2b).

Semedo et al. (2012) found that the annual and seasonal mean Hs are projected to have increased and decreased over large areas of the global ocean by the end of the twenty-first century because of global warming. They encounter predominant decreases at lower latitudes, while at higher latitudes, especially in the Southern Hemisphere, an increase is found. Our results differ from these conclusions, showing lower latitudes with increasing Hs during the last two decades, in the annual trends and also the seasonal, with the exception of DJF season. Also, higher latitudes show a small number of significant increasing linear trends, not consistent through all seasons.

Hemer et al. (2010) build a monthly mean Hs time series by merging satellite data and correlated it with the Southern Oscillation Index. According to this work, the Southern Region is positively correlated with the SOI in Autumn and Winter. On the other hand, the correlation with the Annular Mode Index is throughout the year, extensive to the Northern Region in Winter, although never significant for the Central Region. The authors show also linear trends for significant wave height of the Southeastern Pacific Ocean, with significant positive values of around 0.05 m year^{-1} (0.5 m dec^{-1}) in October, consistent with the values found in this analysis. The monthly trend approach and the inconsistency of the time series length between both analyses make difficult further comparisons.

References

Aguirre C, Rutllant JA, Falvey M (2017) Wind waves climatology of the Southeast Pacific Ocean. Int J Climatol 37(12):4288–4301

Barstow SF (1996) World wave atlas. AVISO Newsletter, No. 4, AVISO, Ramonville St-Agne, France, 24–35

Caires S, Sterl A (2003) Validation of ocean wind and wave data using triple collocation. J Geophys Res 108:3098

Chen G, Chapron B, Ezraty R, Vandemark D (2002) A global view of swell and wind sea climate in the ocean by satellite altimeter and scatterometer. J Atmos Ocean Technol 19(11):1849–1859

Gulev SK, Grigorieva V (2006) Variability of the winter wind waves and swell in the North Atlantic and North Pacific as revealed by the voluntary observing ship data. J Clim 19(21):5667–5685

Hemer MA, Church JA, Hunter JR (2010) Variability and trends in the directional wave climate of the Southern Hemisphere. Int J Climatol 30(4):475–491

Hirsch R, Slack J, Smith R (1982) Techniques of trend analysis for monthly water quality data. Water Resour Res 18:107–121

Kushnir Y, Cardone VJ, Greenwood JG, Cane MA (1997) The recent increase in North Atlantic Wave Heights. J Clim 10(8):2107–2113

Queffeulou P Merged altimeter data base, an update. In: Proceedings of ESA. Living Planet Symposium, 9-13 September 2013, Edinburgh, UK

Queffeulou P, Croizé-Fillon D Global altimeter SWH data set, version 10. Tech. Rep. 2013, Laboratoire d'Océanographie Spatiale, IFREMER

Reyers M, Moemken J, Pinto JG (2016) Future changes of wind energy potentials over Europe in a large CMIP5 multimodel ensemble. Int J Climatol 36(2):783–796

Semedo A, Sušelj K, Rutgersson A, Sterl A (2011) A global view on the wind sea and swell climate and variability from ERA-40. J Clim 24(5):1461–1479

Semedo A, Weisse R, Behrens A, Sterl A, Bengtsson L, Günther H (2012) Projection of global wave climate change toward the end of the twenty-first century. J Clim 26(21):8269–8288

Stopa JE, Cheung KF (2014) Intercomparison of wind and wave data from the ECMWF reanalysis interim and the NCEP climate forecast system reanalysis Ocean. Model. 75:65–83

Wang XL, Feng Y, Swail VR (2014) Changes in global ocean wave heights as projected using multimodel CMIP5 simulations Geophys. Res Lett 41:1026–1034

Young IR, Ribal A (2019) Multi-platform evaluation of global trends in wind speed and wave height. Science 364:548–552. https://doi.org/10.1126/science.aav9527

Young IR, Zieger S, Babanin AV (2011) Global trends in wind speed and wave height. Science 332(6028):451–455